Electronic Supplementary Information

Hybridizing germanium anodes with polysaccharide-derived nitrogen-doped carbon for high volumetric capacity of Li-ion batteries

Jaegeon Ryu,‡[a] *Dongki Hong,*‡[a] *Sunghee Shin,*[a] *Wooyoung Choi,*[a] *Ahyoung Kim,*[a] *and Soojin Park**[a]

[a] Department of Energy Engineering, School of Energy and Chemical Engineering, Ulsan National Institute of Science and Technology (UNIST), Ulsan 44919, South Korea

*Corresponding Authors:

Soojin Park, spark@unist.ac.kr

‡ These authors contributed equally to this work.

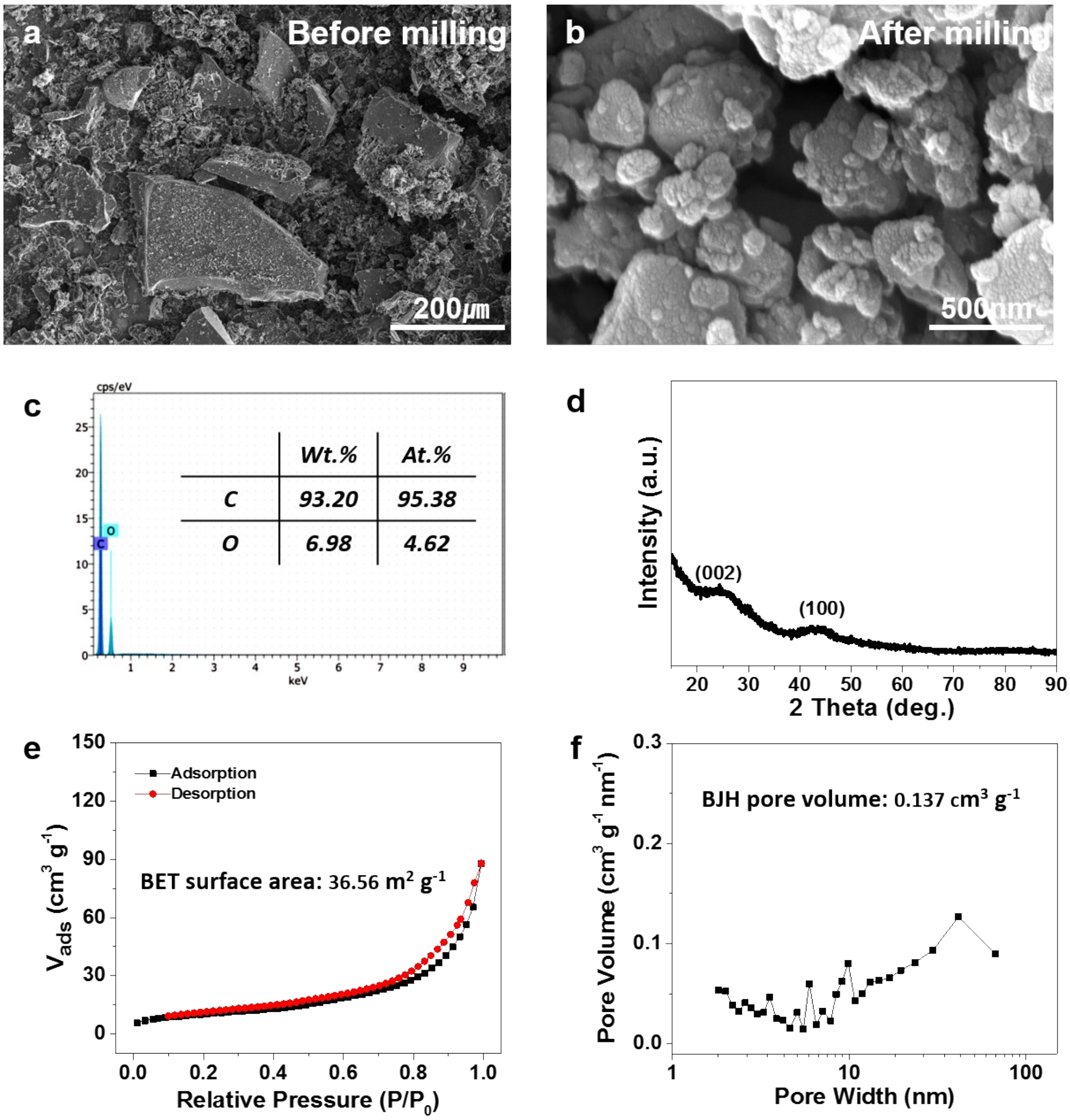

Figure S1. Characterization of AHC. SEM images (a) before and (b) after ball-milling. (c) EDX spectrum and compositional result and (d) XRD pattern of AHC. (e) Nitrogen adsorption isotherms and (f) BJH pore size distribution curve of AHC.

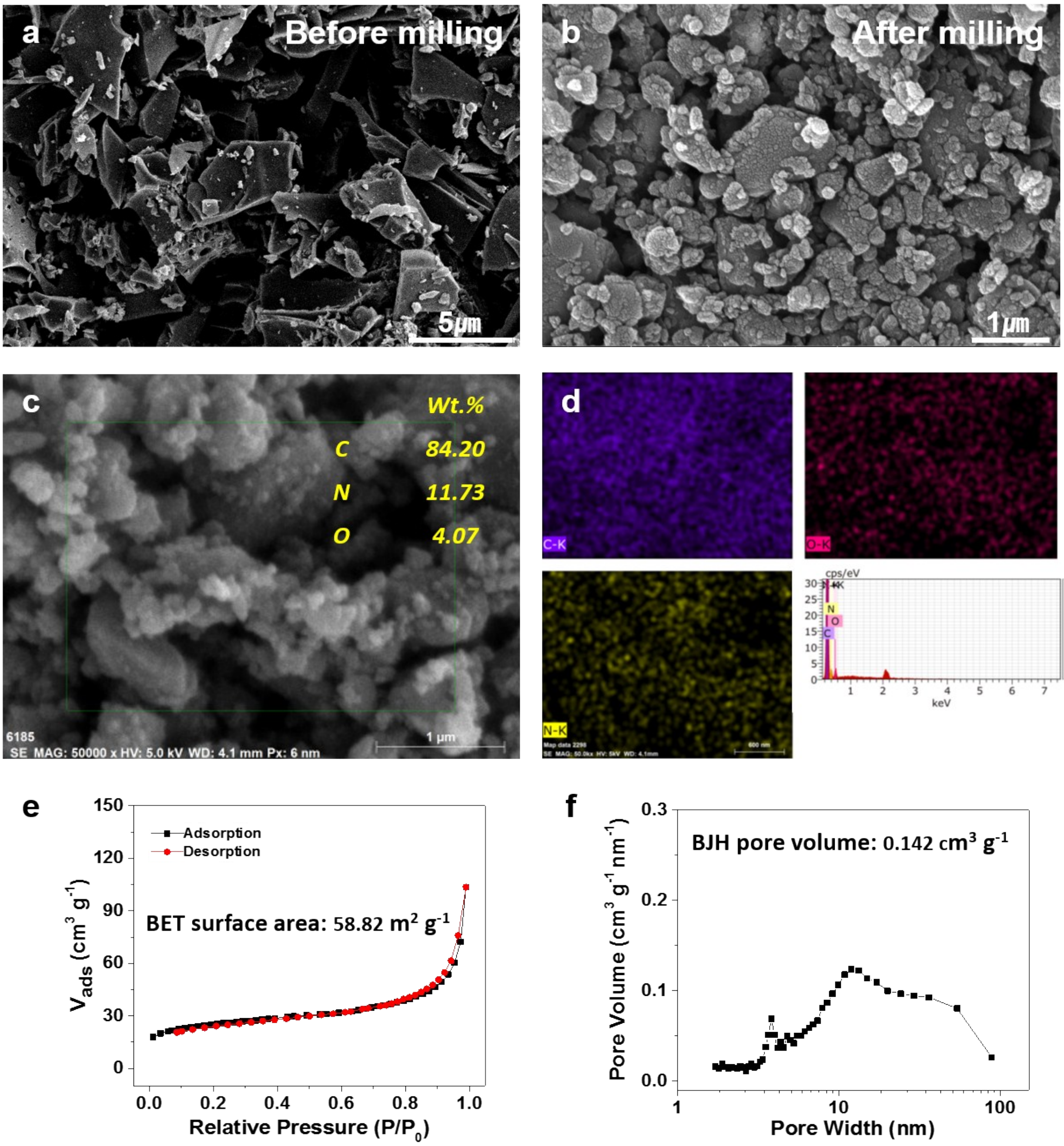

Figure S2. Characterization of ANHC-10. SEM images (a) before and (b-c) after ball-milling. (d) EDS spectrum, compositional result and elemental mapping results. (e) Nitrogen adsorption isotherms and (f) BJH pore size distribution curve of ANHC-10.

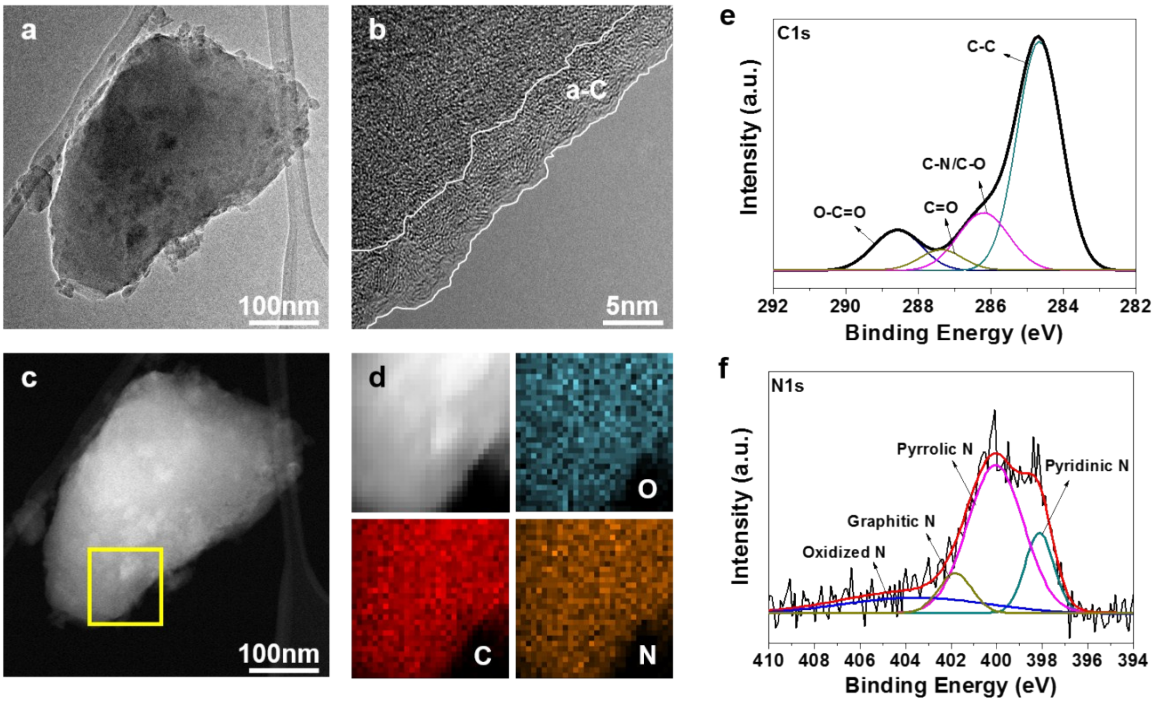

Figure S3. (a-b) TEM images, (c) STEM-HAADF image and (d) EDS elemental mapping results of ANHC-10. XPS spectrum for carbon 1s (e) and nitrogen 1s (f) of ANHC-10.

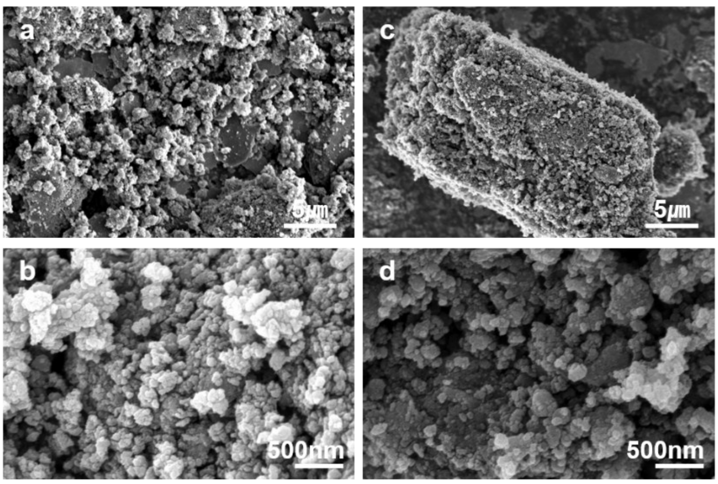

e

Wt.%		*C*	*O*	*N*
AHC	**XPS**	-	-	-
	EDS	93.2	6.98	-
	EA	94.1	5.9	-
ANHC -1	**XPS**	93.3	5.74	0.96
	EDS	92.3	6.18	1.52
	EA	90.8	8.00	1.20
ANHC -5	**XPS**	88.01	7.66	4.33
	EDS	87.2	6.82	5.98
	EA	87.8	7.19	5.01
ANHC-10	**XPS**	86.9	4.12	8.98
	EDS	84.2	4.07	11.73
	EA	85.7	4.26	10.04

Figure S4. Control of nitrogen-doping level. SEM images of (a, b) ANHC-1 and (c, d) ANHC-5. (e) Summary of compositional analysis of AHC-based materials by XPS, EDX and EA.

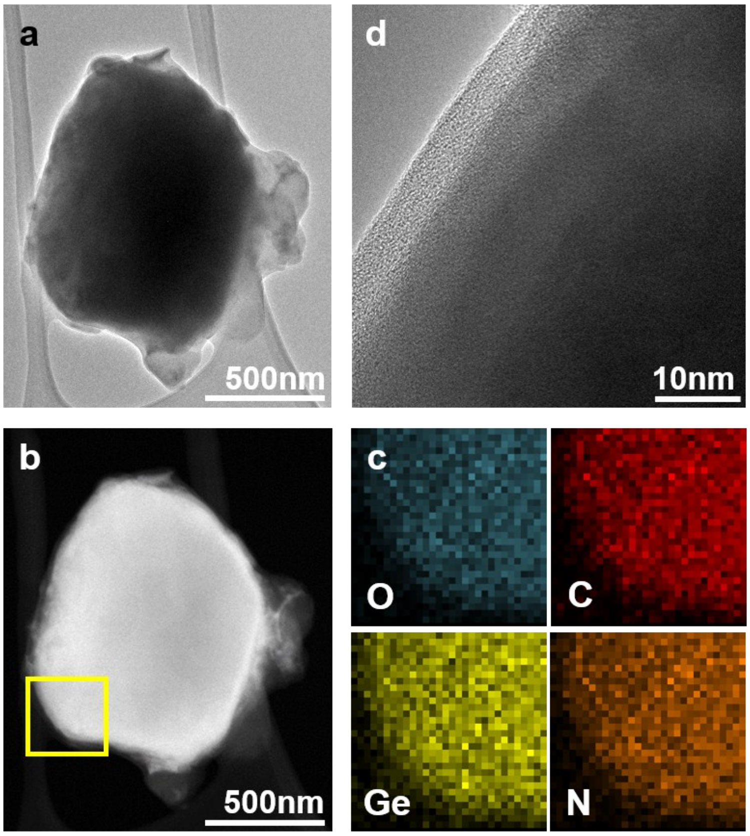

Figure S5. Characterization of ANHC/GeO_2. (a,d) TEM images and (b) STEM-HAADF image of ANHC/GeO_2. (c) EDS elemental mapping results of selected area from the yellow box in (b).

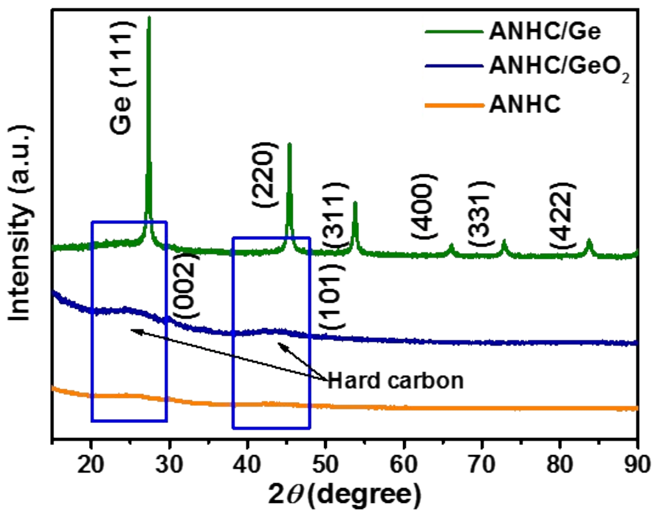

Figure S6. XRD patterns of ANHC, ANHC/GeO_2 and ANHC/Ge.

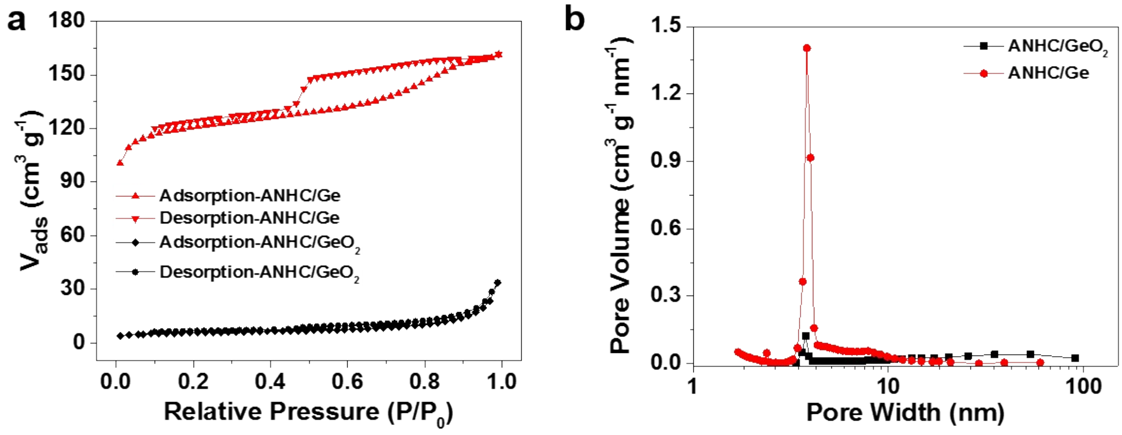

Figure S7. (a) Nitrogen adsorption isotherms and (b) BJH pore size distribution curve of ANHC/GeO_2 and ANHC/Ge.

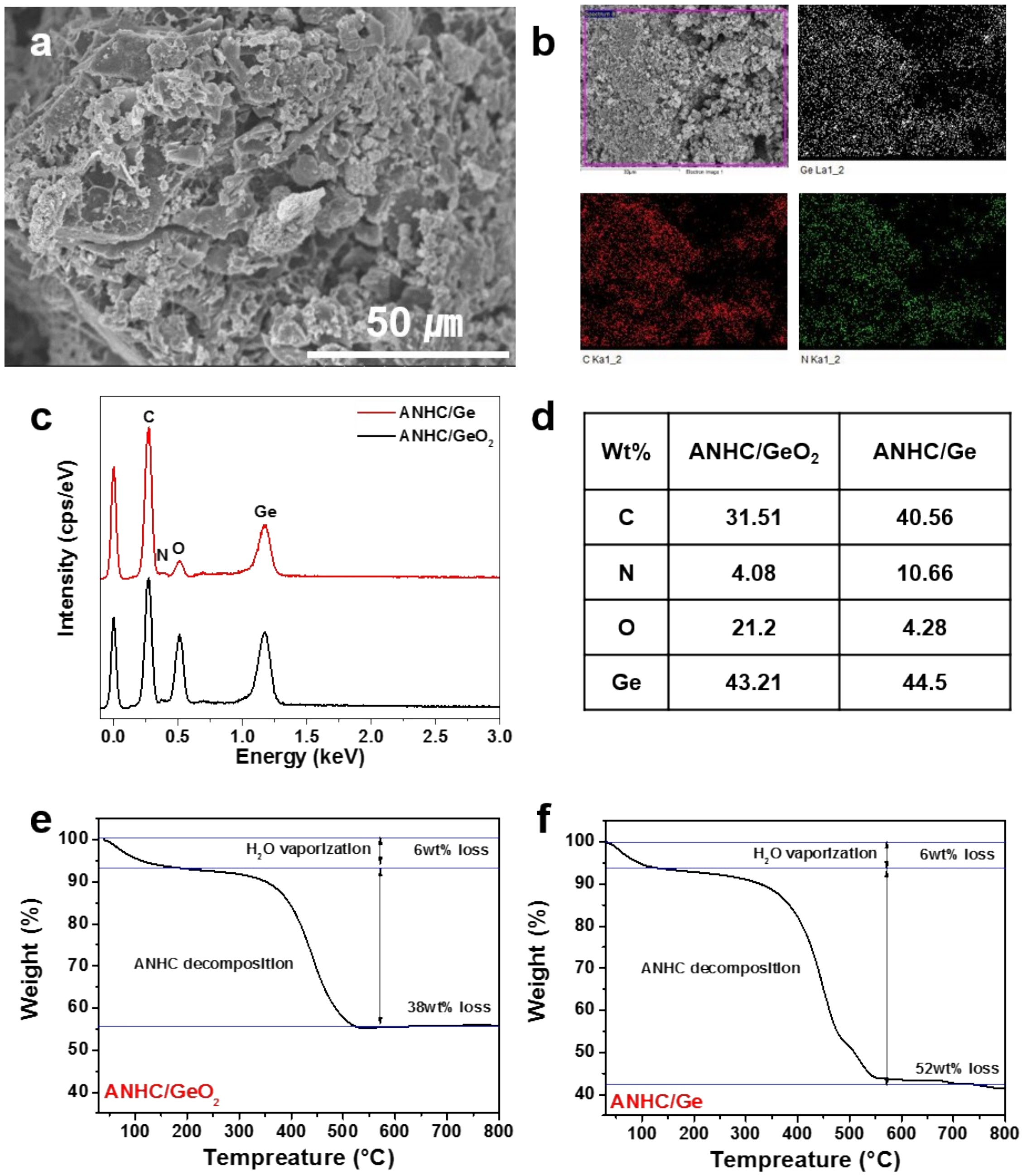

Wt%	ANHC/GeO_2	ANHC/Ge
C	31.51	40.56
N	4.08	10.66
O	21.2	4.28
Ge	43.21	44.5

Figure S8. (a-b) Low magnified SEM image and corresponding EDS mapping results for ANHC/Ge. (c) EDX spectrum, (d) elemental composition results, and (e-f) TGA curves for ANHC/GeO_2 and ANHC/Ge, respectively.

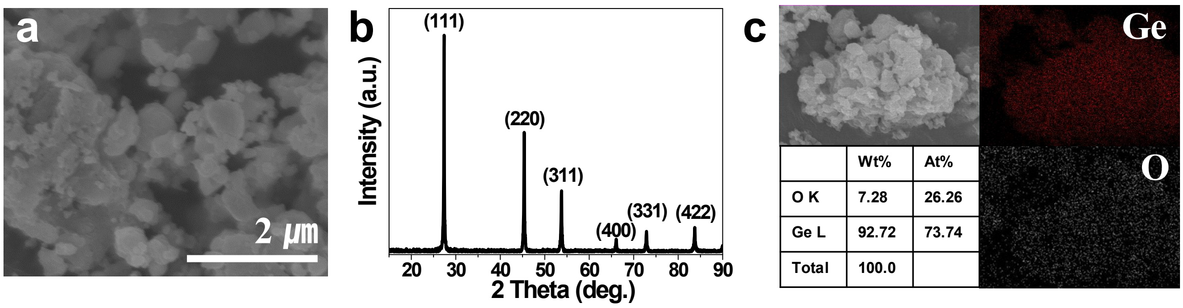

Figure S9. (a-c) SEM image, XRD pattern, and corresponding EDS mapping results for pure Ge.

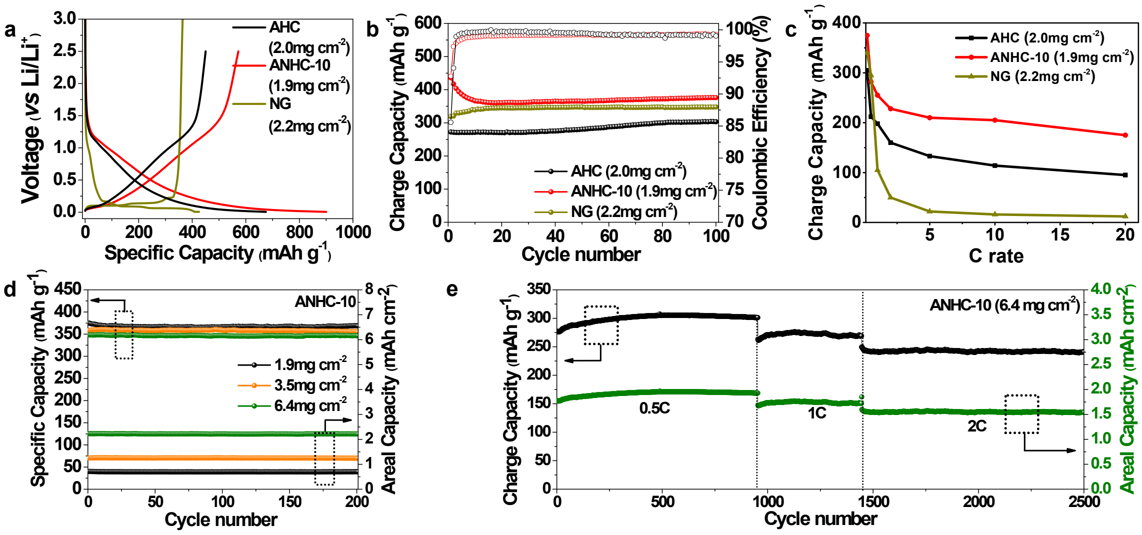

Figure S10. (a) First galvanostatic discharge/charge curves, (b) cycling stability for 100 cycles at a rate of C/2, and (c) charge capacity plots at different C rates for natural graphite (NG), AHC, and ANHC-10 electrodes. (d) Cycling stability for 200 cycles at a rate of 1C with different loading levels. (e) Long-term stability of ANHC-10 electrode with 6.4 mg cm^{-2} loading for 2500 cycles.

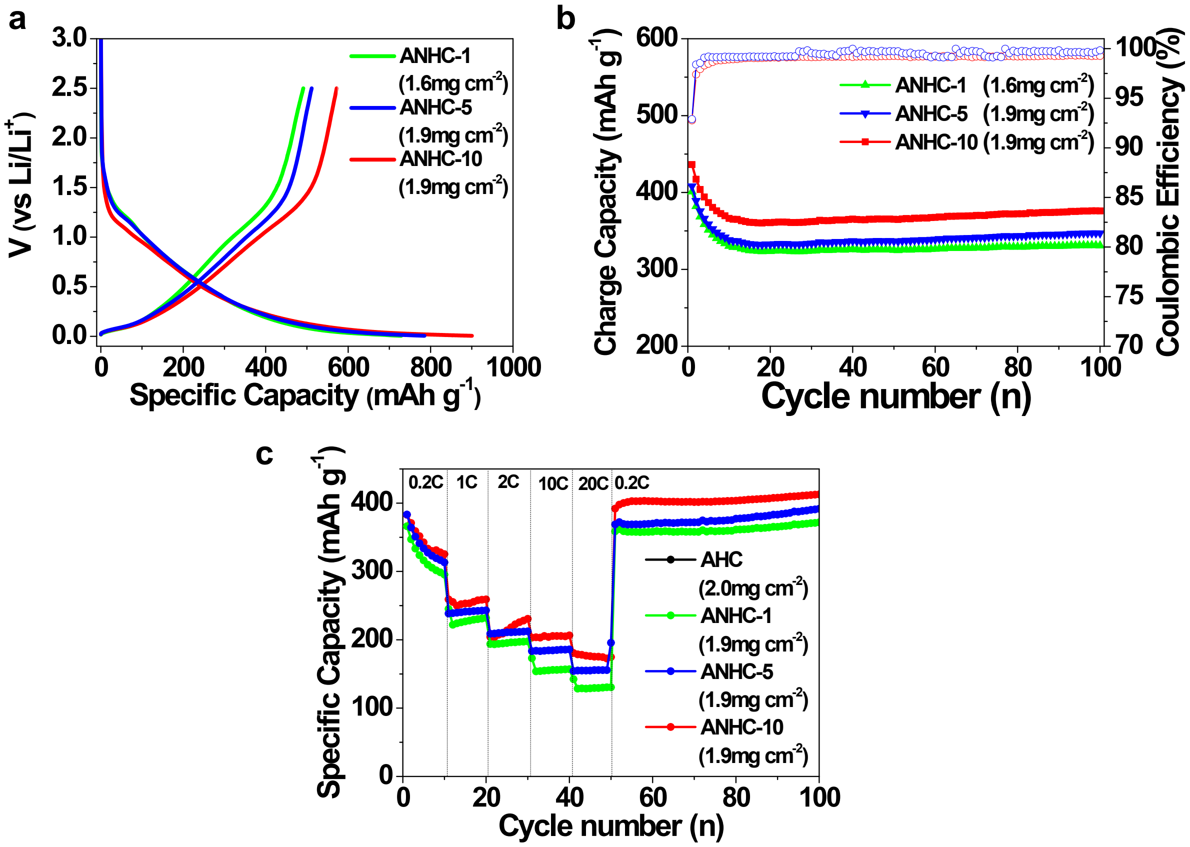

Figure S11. (a) First galvanostatic discharge/charge curves, (b) cycling stability for 100 cycles at a rate of C/2, and (c) rate capabilities of ANHC electrodes with different doping levels.

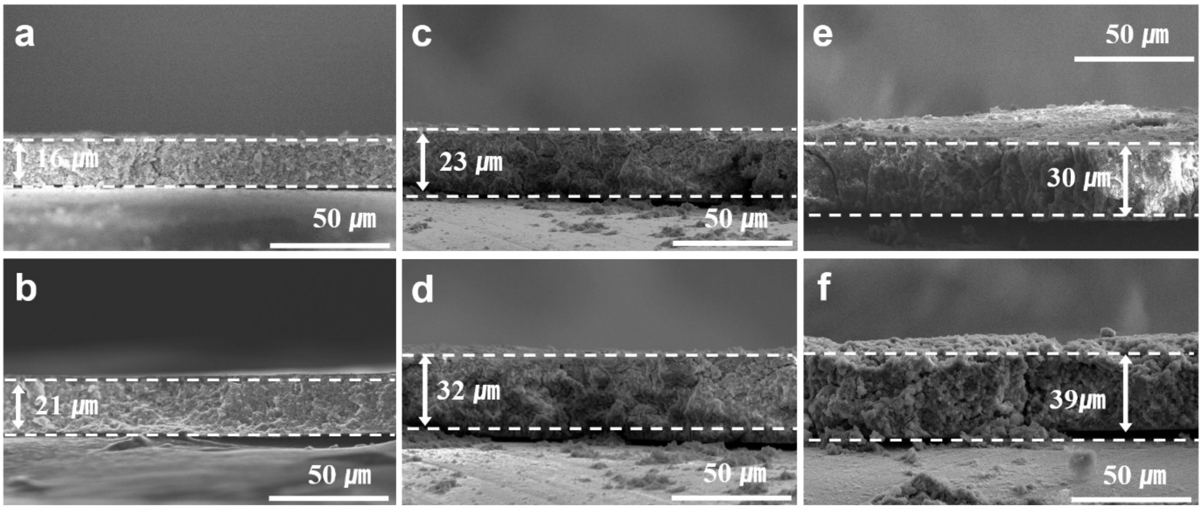

	ANHC-10		
	1.9 mg cm^{-2}	**3.5 mg cm^{-2}**	**6.4 mg cm^{-2}**
Packing density (g/cc)	1.19	1.52	1.88
Electrode Thickness (μm)			
Pristine	16	23	30
After 100 cycles	21	32	39
Expansion (%)	31	39	30
Volumetric capacity (mAh cm^{-3})			
Pristine	568	591	743
After 100 cycles	433	425	571

Figure S12. Electrode swelling results and calculation of volumetric capacities of ANHC electrodes with different loading levels of (a-b) 1.9 mg cm^{-2}, (c-d) 3.5 mg cm^{-2}, (e-f) 6.4 mg cm^{-2}, and their summarized table.

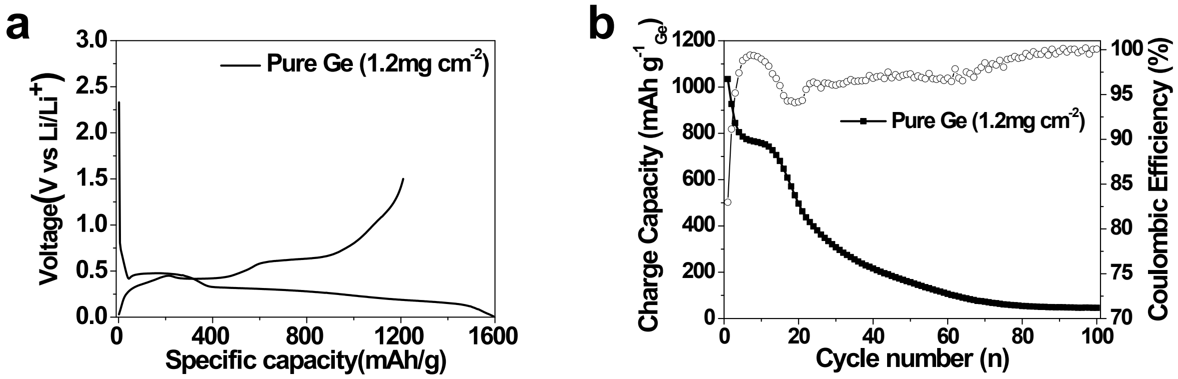

Figure S13. (a) First galvanostatic discharge/charge curves, (b) cycling stability for 100 cycles at a rate of C/2.

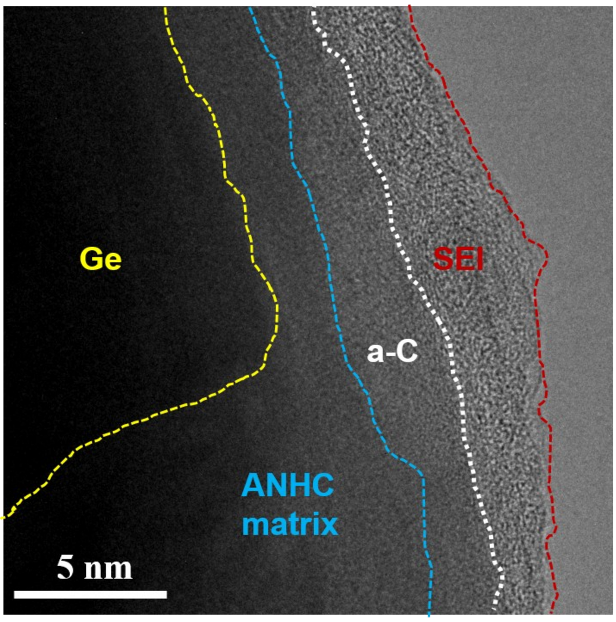

Figure S14. High magnification TEM image of ANHC/Ge after 100 cycles.

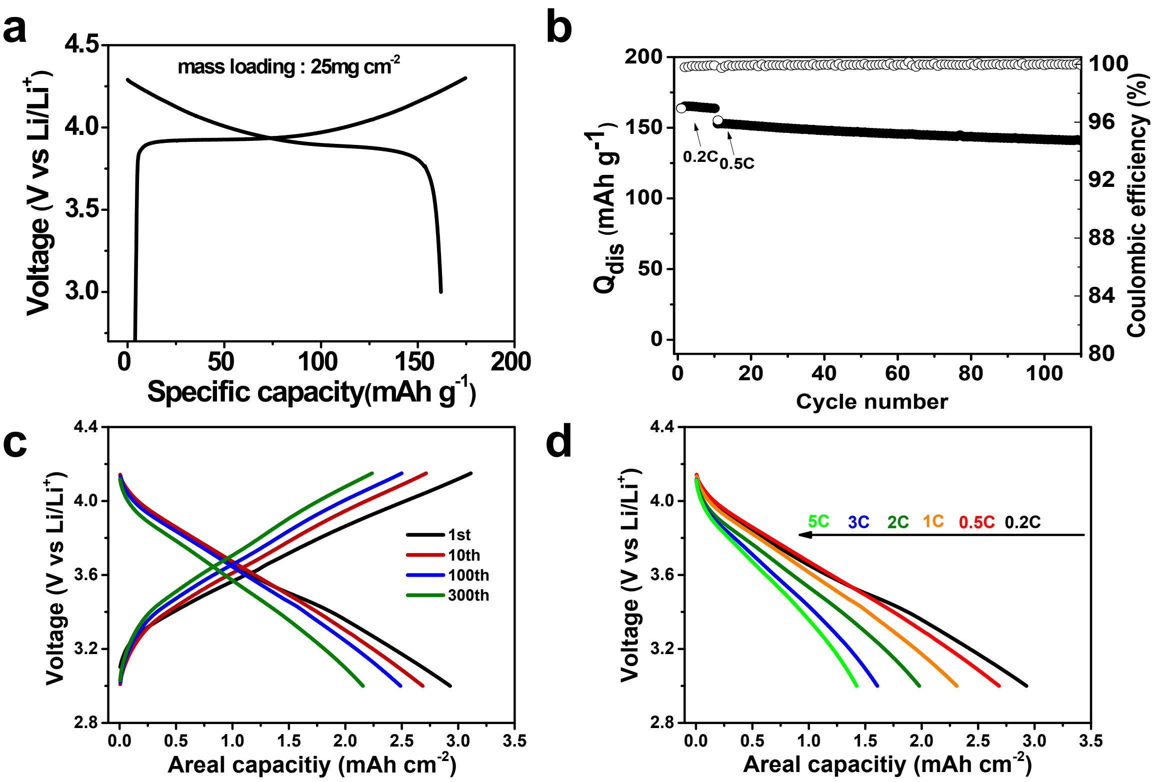

Figure S15. (a) First charge/discharge curve and (b) cycle performance of LCO cathode. (c) Voltage profiles of full cell at different stage of cycling and (d) rate performance of full cell at different rates.

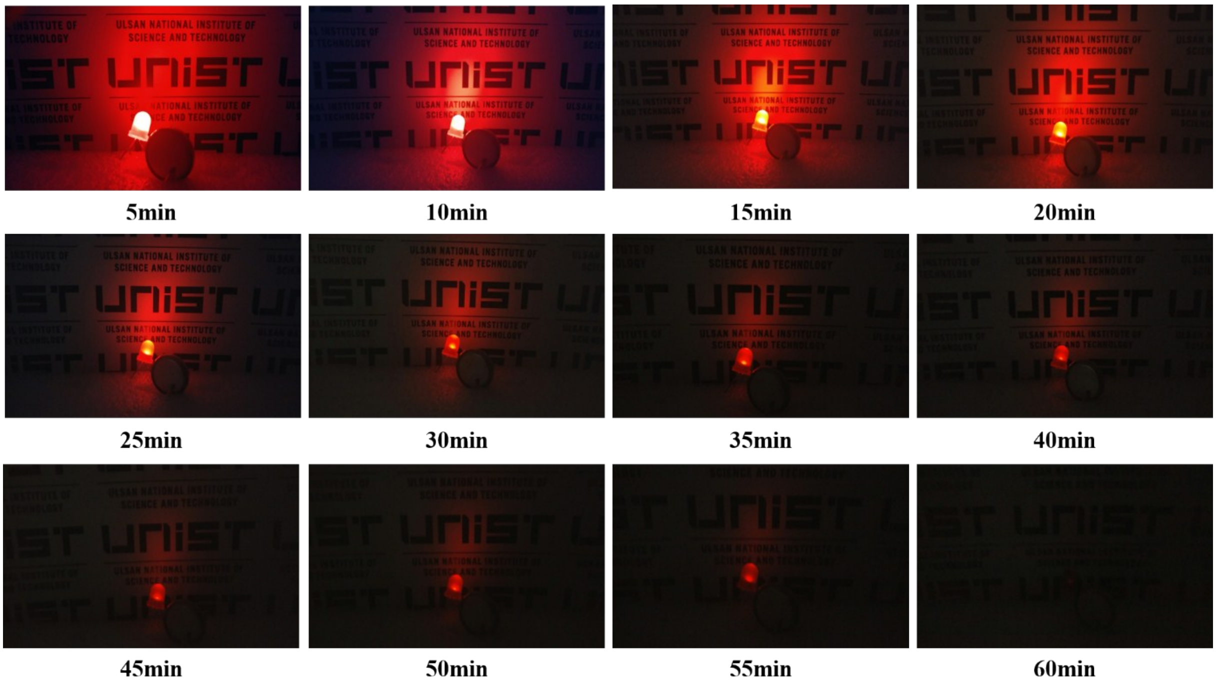

Figure S16. Photographs of Li-ion battery composed of ANHC/Ge anode and LCO cathode (7.62mAh) to light up a red LED bulb requiring a current of 20 mA with an operating voltage of 1.9V; after 5min to time of turn-off.

Table S1. Summary chart for electrochemical performance of various types of anodes including alloy-type anodes and recently reported high volumetric capacity anodes.

Samples	Loading level (mg cm^{-2})	Current density (mA cm^{-2})	Areal capacity (mAh cm^{-2})	Volumetric capacity (mAh cm^{-3} (for X cycles))		Ref
				Half cell	Full cell	
ANHC/Ge	2.25	~1.7	~1.8	~1052 (500)	-	This work
	4.36	~3	~3	~1570 (500)	~288 (300)	
NHGM	2.75	0.1	2.68	1052 (1200)	Not evaluated	53
Si pomegranate	1.93	0.5	~2	~1270 (160)	Not evaluated	1*
Si-ATO	~2	~1.5	~3	~1000 (50)	~270 (100)[a]	2*
Si@Graphene	1.2	~1.5	~3	~2500 (100)	~257 (200)	3*
SGC	6.5	0.31	~3.3	~738 (100)	~292 (100)	4*
Si@C@Graphene	~3.6	~1.5	~2.88	~1100 (1000)	~253 (100)	5*
Macro-Ge	0.8-1.4	1.5	1.2-2.1	~3000 (3000)[c]	N/A	6*

*Supplementary references

[a]This value does not include thickness of current collectors

[b]This value does not include thickness of cathode and current collectors

[c]This paper does not provide any information on the thickness of electrode or calculation method

References

1 N. Liu, Z. D. Lu, J. Zhao, M. T. McDowell, H. W. Lee, W. T. Zhao and Y. Cui, *Nat. Nanotechnol.,* 2014, 9, 187.

2 J. I. Lee, E. H. Lee, J. H. Park, S. Park and S. Y. Lee, *Adv. Energy Mater.,* 2014, 4, 1301542.

3 I. H. Son, J. H. Park, S. Kwon, S. Park, M. H. Rummeli, A. Bachmatiuk, H. J. Song, J. Ku, J. W. Choi, J. M. Choi, S. G. Doo and H. Chang, *Nat. Commun.,* 2015, 6, 7393.

4 M. Ko, S. Chae, J. Ma, N. Kim, H. W. Lee, Y. Cui and J. Cho, *Nat. Energy,* 2016, 1, 16113.

5 X. Zhao, M. Li, K. H. Chang and Y. M. Lin, *Nano Res.,* 2014, 7, 1429-1438.

6 J. Liang, X. Li, Z. Hou, T. Zhang, Y. Zhu, X. Yan and Y. Qian, *Chem. Mater.,* 2015, 27, 4156-4164.